Journal of Extracellular Vesicles

ISSN: (Print) (Online) Journal homepage: https://www.tandfonline.com/loi/zjev20

Exosomal PD-L1 functions as an immunosuppressant to promote wound healing

Dandan Su , Hsiang-I Tsai , Zhanxue Xu , Fuxia Yan , Yingyi Wu , Youmei Xiao , Xiaoyan Liu , Yanping Wu , Sepideh Parvanian , Wangshu Zhu , John E. Eriksson , Dongqing Wang , Haitao Zhu , Hongbo Chen & Fang Cheng

To cite this article: Dandan Su , Hsiang-I Tsai , Zhanxue Xu , Fuxia Yan , Yingyi Wu , Youmei Xiao , Xiaoyan Liu , Yanping Wu , Sepideh Parvanian , Wangshu Zhu , John E. Eriksson , Dongqing Wang , Haitao Zhu , Hongbo Chen & Fang Cheng (2020) Exosomal PD-L1 functions as an immunosuppressant to promote wound healing, Journal of Extracellular Vesicles, 9:1, 1709262, DOI: 10.1080/20013078.2019.1709262

To link to this article: https://doi.org/10.1080/20013078.2019.1709262

Published online: 27 Dec 2019.

JOURNAL OF EXTRACELLULAR VESICLES
2020, VOL. 9, 1709262
https://doi.org/10.1080/20013078.2019.1709262

Taylor & Francis
Taylor & Francis Group

RESEARCH ARTICLE

OPEN ACCESS Check for updates

Exosomal PD-L1 functions as an immunosuppressant to promote wound healing

Dandan Su[a*], Hsiang-I Tsai[a*], Zhanxue Xu[a*], Fuxia Yan[a], Yingyi Wu[a], Youmei Xiao[a], Xiaoyan Liu[a], Yanping Wu[a], Sepideh Parvanian[b], Wangshu Zhu[c], John E. Eriksson[b], Dongqing Wang[d], Haitao Zhu[d], Hongbo Chen[a] and Fang Cheng[a]

[a]School of pharmaceutical sciences (Shenzhen), Sun Yat-sen University, Shenzhen, China; [b]Faculty of Science and Engineering, Åbo Akademi University, Turku, Finland; [c]Department of Radiology, Sun Yat-sen Memorial Hospital, Sun Yat-sen University, Guangzhou, China; [d]Department of medical imaging, The Affiliated Hospital of Jiangsu University, Zhenjiang, China

ABSTRACT

Excessive and persistent inflammation after injury lead to chronic wounds, increased tissue damage or even aggressive carcinogenic transformation. Effective wound repair could be achieved by inhibiting overactive immune cells to the injured site. In this study, we obtained high concentration of PD-L1 in exosomes from either genetically engineered cells overexpressing PD-L1 or IFN-γ stimulated cells. We found that exosomal PD-L1 is specially bound to PD-1 on T cell surface, and suppressed T cell activation. Interestingly, exosomal PD-L1 promoted the migration of epidermal cells and dermal fibroblasts when pre-incubated with T cells. We further embedded exosomes into thermoresponsive PF-127 hydrogel, which was gelatinized at body temperature to release exosomes to the surroundings in a sustained manner. Of importance, in a mouse skin excisional wound model, exosomal PD-L1 significantly fastened wound contraction and reepithelialization when embedded in hydrogel during inflammation phase. Finally, exosomal PD-L1 inhibited cytokine production of CD8+ T cells and suppressed CD8+ T cell numbers in spleen and peripheral lymph nodes. Taken together, these data provide evidence on exosomal PD-L1 exerting immune inhibitory effects and promoting tissue repair.

ARTICLE HISTORY
Received 3 September 2019
Revised 6 December 2019
Accepted 9 December 2019

KEYWORDS
PD-L1; exosomes; wound healing; immunotherapy; thermoresponsive hydrogel

Introduction

Wound healing in clinical settings relies primarily on enabling the natural course of epidermal tissue regeneration [1–3]. In many cases, the involved processes and the progress of regeneration may be insufficient to save severely injured patients [2,4,5]. Within the first few days after the injury, inflammatory and immune cells are recruited from neighbouring regions or from circulation to the wound site by complement, clotting components, and cytokines to clear the wound of cell debris and bacteria [1,6,7]. Excessive and persistent inflammation underlie impaired healing, and thus inhibiting overactive immune cells to the injured tissue represents a powerful therapeutic of chronic ulcers and inflammatory diseases [8–10].

Recently exosomes, membrane vesicles secreted by many cells, have raised great scientific and clinical interest as they carry diverse cargoes including proteins, lipids and nucleic acids that can be transported and exchanged between cells, and influence various physiological and pathological functions of recipient cells [11–13]. Exosomes have been shown to suppress an overactive immune response by several mechanisms, including suppressing the activity of natural killer cells (NKs) and $CD8^+$ T cells, preventing the differentiation and maturation of dendritic cells (DCs), as well as positively mediating the functions of regulatory T cells (Tregs) [14–19]. Thus, these exosomes have the potential as direct therapeutic agents for tissue regeneration and immune response modulation.

The PD-1/PD-L1 immune checkpoint pathway prevents excessive tissue destruction during inflammatory states [20]. PD-L1 expression is induced by proinflammatory factors in multiple cell types throughout the body [21,22]. By binding to the inhibitory PD-1 receptor on T cells, PD-L1 restrains the production of inflammatory cytokines including interferon-γ (IFN-γ), tumour necrosis factor-α (TNF-α), granzyme B, and perforin of activated effector T cells [23–28]. Thus, PD-L1 provide promising target to control the devastating diseases associated with the chronicity of inflammatory

CONTACT Fang Cheng chengf9@mail.sysu.edu.cn; Hongbo Chen chenhb7@mail.sysu.edu.cn School of pharmaceutical sciences (Shenzhen), Sun Yat-sen University, Shenzhen 518107, China; Haitao Zhu zhht25@163.com The Affiliated Hospital of Jiangsu University, Zhenjiang 212001, China
*These authors contributed equally to this work

This article has been republished with minor changes. These changes do not impact the academic content of the article.

responses. Interestingly, recently PD-L1-positive exosomes are found to be secreted from metastatic human melanoma cells into tumour microenvironment and circulation to suppress the anti-tumour immunity systemically. The PD-1+ CD8+T cells are the primary target cells inhibited by exosomal PD-L1 to dampen the immune pressure at the effector stage. This T cell inhibition can be blocked by antibodies to disrupt the interaction between exosomal PD-L1 and PD-1 on T cells [17]. Thus, we would like to test if exosomal PD-L1 would regulate the immunity and inflammatory response to maintain proper immune homoeostasis during wound healing.

In this study, exosomal PD-L1 were isolated from cells stimulated with IFN-γ or from genetically engineered cells overexpressing PD-L1. We found that exosomal PD-L1 led to decreased T cell proliferation, consequently speeding up skin cell migration *in vitro* and wound healing *in vivo*. In addition, exosomal PD-L1 led to a clear reduction of CD8+ T lymphocytes in the spleen and lymph nodes when incorporated into PF-127 thermoresponsive hydrogel to the mouse skin excisional injury during inflammation phase. These results reveal a novel immunosuppression function of exosomal PD-L1 and provide evidence that boosting the PD-1/PD-L1 immune checkpoint pathway promotes tissue repair and regeneration.

Materials and methods

Cell culture

In order to acquire establishing the stable cell line expressing PD-L1, SK-MEL-5 cells (human melanoma cell line) and B16F10 cells (mouse melanoma cell line) were infected with lentiviruses carrying human/mouse PD-L1 gene (C-OFP Spark tag) (Sino Biological inc). In order to delete PD-L1 in cells, the designed sgRNAs were cloned into the lentiCRISPR v2 (Addgene) according to the previous protocol (the sequences of sgRNA are listed in Table 1) [29]. HEK 293T cells (human embryonic kidney cell line), HaCaT cells (spontaneously immortalized human keratinocyte cell line), HDF cells (primary human dermal fibroblasts cell line), SK-MEL-5 cells and B16F10 cells were cultured in Dulbecco's modified Eagle's medium (DMEM; Gibco) supplemented with 10% foetal bovine serum (FBS; Gibco) and 1% (v/v) penicillin/streptomycin (P/S; Gibco) at 37°C in a 5% CO2 atmosphere. Jurkat T cells and Peripheral blood mononuclear cells (PBMCs) were cultured in RPMI 1640 (Gibco) with 10% FBS.

Table 1. The sequences of sgRNA.

sgRNA oligonucleotides:	Sequences:
human *Pd-l1* guide 1:	GGTTCCCAAGGACCTATATG
human *Pd-l1* guide 2:	ACAGAGGGCCCGGCTGTTGA

Isolation of exosomes

Exosomes were purified from the supernatant of SK-MEL-5 cells and B16F10 cells. At 70% confluence, cells were washed three times with PBS, and the culture medium was substituted with a similar volume of DMEM supplemented with 0.5% exosome-free FBS and 1% P/S. For stimulation with IFN-γ, cells were stimulated with 100 ng/ml IFN-γ (PeproTech). After incubating for 48 h, exosomes were purified from the conditioned medium by a differential centrifugation protocol based on a standard literature protocol [30]. All centrifuge processes were performed at 4 °C in order to prevent inactivation of exosomes. In brief, culture supernatants were centrifuged serially at 500 × g for 10 min, 2000 × g for 20 min and 10,000 × g for 40 min to remove cells, dead cells and cell debris (Beckman Coulter, Allegra X-30R), respectively. The supernatants were centrifuged at 100,000 × g for 90 min (Beckman Coulter, Optima L-100XP). The pellet was suspended in ice-cold PBS to remove contaminating protein. Exosomes were collected by ultracentrifugation at 100,000 × g for 90 min, and the pelleted exosomes were resuspended in 100 µL ice-cold PBS and stored at −80 °C immediately for future analysis.

Western blotting

The protein concentrations of exosomes derived from SK-MEL-5 cells (*WT*), PD-L1 knockout SK-MEL-5 cells ($Pd\text{-}l1^{-/-}$), IFN-γ-treated SK-MEL-5 cells (*WT+IFN-γ*, $Pd\text{-}l1^{-/-}$*+IFN-γ*) and PD-L1 overexpressing SK-MEL-5 cells (*WT+PD-L1*) were measured by BCA protein assay. Cells and exosomes pellets were lysed in radioimmunoprecipitation assay buffer (RIPA, CWBIO) and incubated at 4°C for 30 min. Equal amounts of protein were separated by 10% SDS-PAGE and transferred onto polyvinylidene fluoride membranes (Millipore, Darmstadt, Germany). Membranes were blocked with 5% non-fat milk for 2 h and incubated with primary antibodies overnight at 4°C. After washing with PBS, membranes were incubated with appropriate secondary antibodies at room temperature for 2 h. Protein bands were visualized with the HRP-enhanced chemiluminescence western blotting substrate (Advansta). The primary antibodies for western blot analysis are shown below: anti-PD-L1 (AbWays technology), anti-CD63 (ExoAb Antibody Kit, SBI), anti-CD81 (ExoAb Antibody Kit,

SBI), anti-Alix (Santa cruza technology), anti-GAPDH (Abmart), anti-β-actin (Abmart). The secondary antibodies were included goat anti-rabbit (ExoAb Antibody Kit, SBI) and goat anti-mouse (Sera care).

Transmission electron microscopy (TEM)

The shape of exosomes derived from SK-MEL-5 cells in the purified samples was observed by transmission electron microscopy. Ten-microlitres purified exosomes were suspended in PBS and placed on formvar-carbon-coated copper grids. After allowing exosomes attached on grids for 10 min, the liquid was removed from the edge of grids by filter paper. Exosomes on the grids were then stained with 2% uranyl acetate for 10 min. Grids were washed with distilled deionized water for 10 min and then air-dried. Exosomes were imaged by TEM (HC-1, Hitachi) at 80 kV.

Analyses of the size and zeta potential of exosomes

Size distributions and Zeta potential of exosomes derived from SK-MEL-5 cells were measured by an instrument (NanoBrook 90Plus PALS, Brookhaven instruments). Exosomes were diluted with PBS at an adjusted concentration of 5 μg/mL and quantified from 0 to 5000 nm. Experiments were repeated three times. Results were expressed as the mean (± SEM).

Immunostaining

For observing PD-L1 expression on cell membrane or on exosomes, cells were first stained with the fluorescent lipophilic tracer Wheat Germ Agglutinin (WGA) CF®488A conjugate dye (Biotium, USA) (5 μg/mL) for 15 min and removed excess dye by washing with PBS. PD-L1 overexpressing exosomes (50 μg/ml) were stained with Cyanine5.5 NHS ester dye (Lumiprobe) (50 μg/mL) and removed excess dye by 100K Amicon® Ultra-15 centrifugal filter devices (Millipore). Cells were incubated with labelled exosomes for 15 min, and then seeded on top of glass coverslips via cytospin. The coverslips were washed as described before and dipped in MilliQ water once. The excess water was removed, the coverslips were mounted on the slides with mowiol and left to dry overnight. The imaging was performed using a ZEISS LSM 880 NLO confocal microscope with multiple objectives.

PBMCs isolation and proliferation

To determine whether exosomal PD-L1 can suppress the proliferation of T cell, the co-incubation experiment was performed. PBMCs were harvested from healthy donor's blood and isolated by Ficoll gradients. PBMCs (8×10^5) were stained with carboxyfluorescein succinimidyl ester (CFSE, a cell division-tracking dye, BioLegend) (5 mM) according to the manufacturer's protocol and placed in wells of 24-well plates. PBMCs were incubated with exosomes (100 μg/ml) derived from SK-MEL-5 cells (*WT*), PD-L1 knockout SK-MEL-5 cells (*Pd-l1*$^{-/-}$), SK-MEL-5 cells treated with IFN-γ (*WT+IFN-γ, Pd-l1*$^{-/-}$*+IFN-γ*), SK-MEL-5 cells expressing exogenous PD-L1 (*WT+PD-L1*) and immunosuppressant FK506 (MedChemExpress) (100 nM) (*FK506* group), supplemented with complete 1640 culture medium for 3 and 7 days. PBMCs were stained with CFSE and cultured with complete 1640 culture medium alone for 0, 3 and 7 days as *Ctrl (d0), Ctrl (d3)* and *Ctrl (d7)* groups, respectively. The proliferation of PBMCs was analysed by flow cytometry (MoFlo High-Performsnce Cell Sorter, Beckman).

Scratch assay

To evaluate whether exosomes can inhibit T cells and promote the migration of skin cells in the immune environment, a scratch assay was implemented. HDF and HaCaT cells were seeded in wells of 24 well plates and cultured with DMEM complete medium. At 70% confluence, cells were scratched using a 200 μL pipette tip and washed with PBS. To mimic the immune environment, cells were cultured with the serum-free medium in addition to the medium in which PBMCs had been cultured (2:1 dilution). Cells were incubated with exosomes (100 μg/mL) from SK-MEL-5 cells (*WT*), PD-L1 knockout SK-MEL-5 cells (*Pd-l1*$^{-/-}$), SK-MEL-5 cells treated with IFN-γ (*WT+IFN-γ, Pd-l1*$^{-/-}$*+IFN-γ*), SK-MEL-5 cells expressing exogenous PD-L1 (*WT+PD-L1*) and bFGF (2.5 ng/ml) (*bFGF*) for 24 h. Cells were cultured in serum-free medium as the negative control (*Ctrl*). The images of the closing area were taken by a microscope (Nikon, Japan) at 0 and 24 h time points. The percentage of migration of the area between wound edges was calculated by ImageJ software.

Preparation of hydrogel containing exosomes

The 25% thermoresponsive Pluronic F-127 hydrogel (PF-127, sigma) was dissolved in sterile PBS by stirred at 4 °C for 2 h. After solubilization, it was sterilized by 0.22 μm filter at 4 °C. Then, exosomes were suspended in PBS and added to the hydrogel making the final concentration of PF-127 hydrogel to 20%.

The rheological property of PF-127 hydrogel

The rheological property of 20% PF-127 hydrogel changes as temperature from 5°C to 40°C was evaluated by the rotational rheometer (Kinexus, Malvern). The samples of PF-127 were prepared in the form of hydrogel, placed in the test area by a spoon and measured with a 25 mm parallel-plate. Twenty per cent PF-127 were cooled to 5°C, the temperature rise rate was 5 °C/min. The elastic moduli (G′) and viscous moduli (G″) were measured at a strain amplitude of 1% and a frequency of 0.159 Hz.

Scanning electron microscopy (SEM)

Twenty per cent PF-127 hydrogel was precooled at −80 °C for 12 h and freeze-dried for 15 h by vacuum freezing drying oven (Alpha 1–4 LDplus, Christ), and then was analysed by SEM (S-3400N, Hitachi).

Exosomes uptake by HaCaT cells in hydrogel condition

Verification of uptake exosomes in 20% PF-127 hydrogel by confocal microscopy. Previously, exosomes in PBS were incubated with WGA 488A dye (5 μg/mL) for 15 min. The stained exosomes were ultrafiltrated by 100K Amicon® Ultra-15 centrifugal filter devices (Millipore). For the hydrogel condition, 20% PF-127 hydrogel-containing stained exosomes (50 μg/ml) were incubated for 10 min at 37°C and then incubated for 10 min at 4°C. Twenty per cent PF-127 hydrogel-containing exosomes were added to the HaCaT cells layer and allowed to gel for 5 min at 37°C. The same volume of serum-free medium was added to the hydrogel layer and incubated at 37°C for 1, 4, 8, 24 and 36 h. HaCaT cells were incubated with serum-free medium alone as the negative control (*Ctrl*). After incubation, the cells were fixed with 4% paraformaldehyde for 20 min followed by three washing steps with PBS. The nuclei of HaCaT cells were labelled with DAPI (Beyotime Biotechnology) at 0.5 μg/mL in PBS for 15 min and washed with PBS. Analyses were carried out by the ZEISS LSM 880 NLO system.

Mouse skin injury experiment

Animal procedures were approved by the Institutional Animal Care and Use Committee (IACUC) at Sun Yat-Sen University (approval number: SYSU-IACUC-2019-000019). Balb/c were obtained from laboratory animal centre of Sun Yat-Sen University. All mice weighing 18–25 g were used in this study. Mice were maintained under specific pathogen-free conditions and housed alone with food and water. These mice were given an intraperitoneal injection of pentobarbital sodium (Sigma-Aldrich) at a dose of 10 ml/kg. Removed the hair from the back of the mice by using hair removal creams. A 10-mm diameter circle was designed on the midline of the mice back spine and then created a standardized full-thickness skin wound. After stopping the bleeding with a cotton swab, the mice were randomly assigned to different treatment groups. Mice were treated with exosomes derived from mouse melanoma B16F10 cell line. *WT* (1 μg/μL), *WT +IFN-γ* (1 μg/μL), *WT+PD-L1* (1 μg/μL) and *bFGF* (0.5 ng/μL) were embedded with 20% PF-127 hydrogel (50 uL) and applied on the wounds, which was gelatinized at body temperature to preserve exosomes throughout the wound. The negative group was treated with 20% PF-127 alone (*Ctrl*). All the mice were treated once daily from day 3 until day 7. The damaged skin, spleen and lymph nodes were removed from the sacrificed mice on day 7 for further analysis. All mice were monitored daily for changes in body weight and wounds. The wound area was measured using ImageJ software.

Histology and immunohistochemistry analysis

Three wounds per group were performed for macroscopic evaluation by histopathological analysis on day 7. The skin was fixed in 4% paraformaldehyde overnight, dehydrated through a graded series of ethanol, embedded in paraffin, cut into slices and stained by haematoxylin and eosin (H&E). For immunohistochemistry analysis, sections from selected paraffin blocks were deparaffinized through xylene and a graded series of ethanol and then blocked endogenous peroxidase activity by incubating sections in 3% H_2O_2 solution. After blocking with 10% goat serum mixture, these slides were incubated with primary antibodies and secondary antibodies. The primary antibodies were anti-Ki67, anti-alpha smooth muscle (α-SMA), anti-Vimentin (Monoclonal Mouse, ServiceBio). Finally, slides were incubated with DAB substrate solution to reveal the colour of antibody staining and counterstained with haematoxylin for visualization and quantification.

RNA isolation and qPCR analysis

The total RNA was collected and purified from cells and skin tissue by TRIZOL reagent (TaKaRa, Tokyo, Japan) according to the manufacturer's protocol. The skin tissue was ground down in the mortar before adding TRIZOL reagent. RNA concentration was measured by NANODROP ONE (Thermo Fisher Scientific). RNA was reversely transcribed into complementary DNA

Table 2. The sequences of the qPCR primers.

Gene	Forward primer sequence 5′→3′	Reverse primer sequence 5′→3′
Human-β-Actin	CCACACTGTGCCCATCTAC	AGGATCTTCATGAGGTAGTCAGTC
Human PD-L1	TCCACTCAATGCCTCAAT	GAAGACCTCACAGACTCAA
Mouse-β-Actin	GGCTGTATTCCCCTCCATCG	CCAGTTGGTAACAATGCCATGT
Mouse-TNF-α	CATCCTTGCGAGTGTCAGTGA	CCCTCACACTCAGATCATCTTCT
Mouse-Granzyme B	TCTCGACCCTACATGGCCTTA	TCCTGTTCTTTGATGTTGTGGG
Mouse-IL-6	CCTCTGGTCTTCTGGAGTACC	ACTCCTTCTGTGACTCCAGC

(cDNA) by using HiScript III RT SuperMix for qPCR (+gDNA wiper) (Vazyme, China) with T100TM Thermal Cycler (BIO-RAD), and then quantified by qPCR using 2x SYBR Green qPCR Mix (ES Science, China) with LightCycler® 96 (Roche). All processes were performed by the manufacturer's instructions. Relative gene expression folding changes were identified with the $2^{-\Delta\Delta Ct}$ method. The primers used in this study are summarized in Table 2.

Cell preparation for flow cytometry

In order to analyse the CD4+ and CD8 + T cell content in mouse spleen and lymph nodes during wound healing, the spleen and lymph nodes of the sacrificed mice on day 7 were removed in a sterile environment, washed with PBS, and then ground on a 0.75-μm sieve. The obtained cell suspension was washed with PBS, centrifuged at 1000 rpm for 5 min and then lysed with red blood cell lysis buffer (Solarbio). The cells were stained with cell staining buffer (Biolegend), incubated with antibodies of APC anti-mouse CD4 (BioLegend), brilliant violet 510™ anti-mouse CD8 (BioLegend), FITC anti-mouse CD3 (BioLegend) and finally analysed by flow cytometry (MoFlo High-Performance Cell Sorter, Beckman).

Statistical analysis

All the statistical analyses were performed with GraphPad Prism 7 (GraphPad Software Inc., USA) and Origin pro 2018 software. Three independent sample replicates were carried out for each experiment unless it was stated otherwise. The statistical significance between the two groups was measured by using the unpaired Student's t-test. All data were expressed as mean ± standard error of the mean (SEM, n = 3), except the quantitation of CD8+T cells from mice, which were expressed as mean ± standard deviation (SD). P-values < 0.05 were considered to be significant (* indicate P < 0.05, * * indicate P < 0.01, and * * * indicate P < 0.001).

Results

PD-L1 packaged in melanoma cell-derived exosomes

It has been reported that PD-L1 presents on surfaces of both cancer cells and derived exosomes, especially in response to IFN-γ stimulation [17]. To test if overexpressing PD-L1 in cancer cells also increase the secretion of PD-L1 in exosomes, we infected the human melanoma cells SK-MEL-5 with lentiviruses to get a stable cell line expressing human PD-L1. qPCR data showed a 46.7-fold increase of PD-L1 mRNA levels in lentivirus-infected cells (*WT+PD-L1*) and a 11.2-fold increase in IFN-γ-treated cells (*WT+IFN-γ*) compared to untreated SK-MEL-5 cells (*WT*) (Figure 1(a)). Western analysis showed similar upregulation of cellular PD-L1 protein levels in *WT+PD-L1* and *WT+IFN-γ* cells (Figure 1(b)). To control the effect of other immune-related proteins in exosomes, we also established a PD-L1 knockout SK-MEL-5 cell line ($Pd\text{-}l1^{-/-}$) and confirmed the loss of PD-L1 by qPCR and western blotting with or without IFN-γ treatment (($Pd\text{-}l1^{-/-}$+*IFN-γ* and $Pd\text{-}l1^{-/-}$) (Figure 1(a,b)). We then purified exosomes derived from these cells by differential centrifugation and confirmed the presence of PD-L1 protein in the exosomes, indicated by exosomal markers CD81, CD63 and Alix in isolated vesicles (Figure 1(b)). IFN-γ or PD-L1 overexpression enhanced PD-L1 level in exosomes (Figure 1(b)), but the total protein amount was almost identical in all types of exosomes (Figure 1(c)), confirming that similar to the cell-surface membrane PD-L1, exosomal PD-L1 increases in response to IFN-γ or PD-L1 overexpression. The TEM images showed that majority of exosome vesicles were round-shaped and membrane-bounded (Figure 1(d)). According to dynamic light scattering (DLS) analysis, exosomes from SK-MEL-5 cells (*WT*), PD-L1 knockout SK-MEL-5 cells ($Pd\text{-}l1^{-/-}$), IFN-γ treated SK-MEL-5 cells (*WT+IFN-γ*, $Pd\text{-}l1^{-/-}$+*IFN-γ*) and PD-L1 overexpressing SK-MEL-5 cells (*WT+PD-L1*) displayed a similar size distribution, with similar mean Zeta potential (−26.54 ± 0.75, −26.61 ± 1.84, −28.09 ± 0.55, −26.40 ± 0.80, −27.33 ± 0.82) (Figure 1(e,f)).

Exosomal PD-L1 suppressed T cell activation and promoted skin cell migration in vitro

To test if PD-L1 overexpressing exosomes physically interact with PD-1 on cell surface, exosomes derived

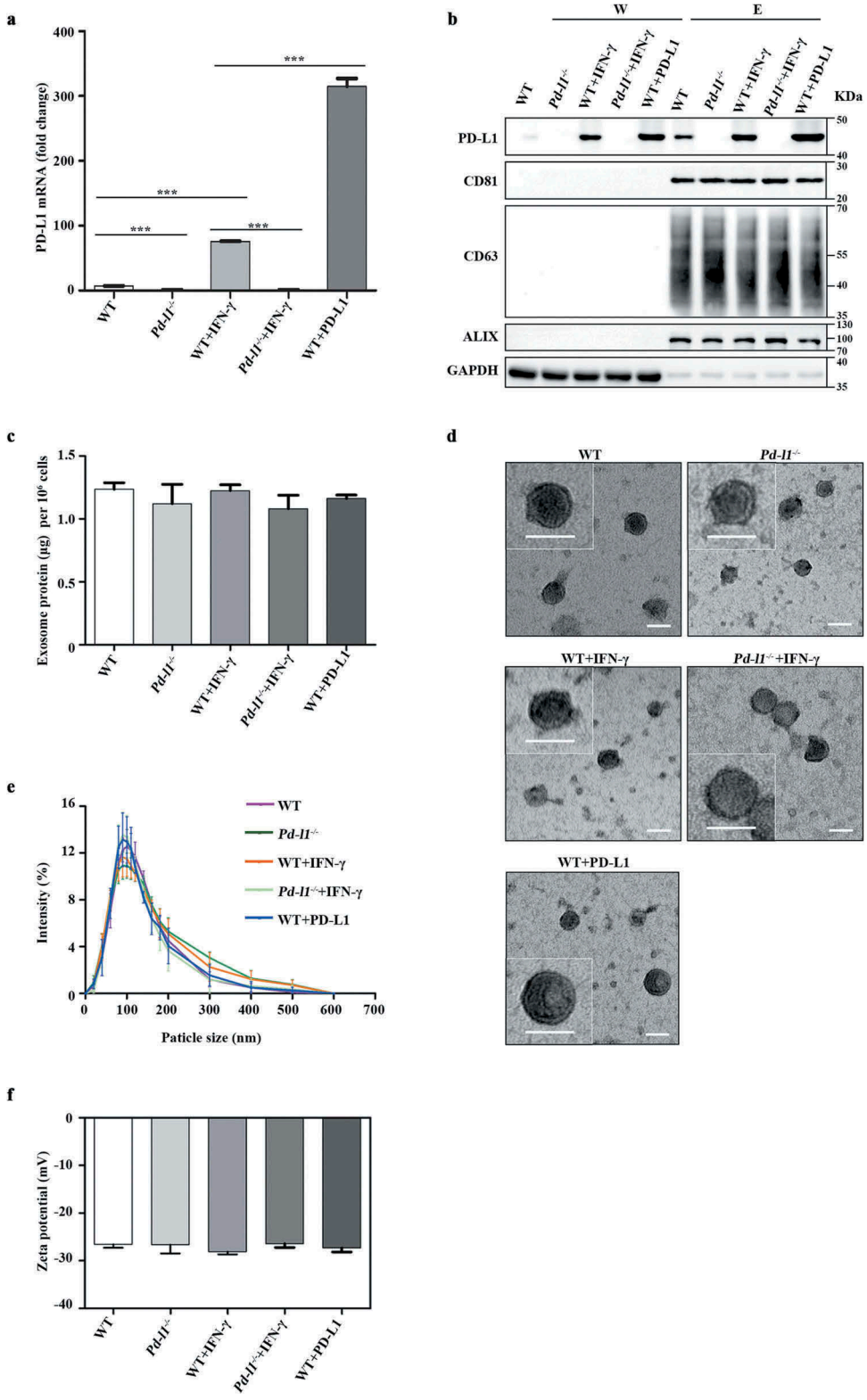

Figure 1. Characterization of exosomes purified from melanoma cells (a). qPCR of PD-L1 mRNA levels in SK-MEL-5 cells (*WT*), PD-L1 knockout SK-MEL-5 cells (*Pd-l1*$^{-/-}$), IFN-γ treated cells (*WT+IFN-γ*, *Pd-l1*$^{-/-}$*+IFN-γ*) and PD-L1 overexpressing cells (*WT+PD-L1*). n = 3. (b). Western blot for PD-L1, CD81, CD63, ALIX and GAPDH in the whole cell lysate (W) and purified exosomes (E) from *WT*, *Pd-l1*$^{-/-}$, *WT+IFN-γ*, *Pd-l1*$^{-/-}$*+IFN-γ* and *WT+PD-L1*. (c). The protein yield of exosomes from *WT*, *Pd-l1*$^{-/-}$, *WT+IFN-γ*, *Pd-l1*$^{-/-}$ *+IFN-γ* and *WT+PD-L1*. n = 3. (d). TEM images of purified exosomes from *WT*, *Pd-l1*$^{-/-}$, *WT+IFN-γ*, *Pd-l1*$^{-/-}$*+IFN-γ* and *WT+PD-L1*. Scale bar: 50 nm. (e-f). The size distribution (e) and the Zeta potential (f) of exosomes from *WT*, *Pd-l1*$^{-/-}$, *WT+IFN-γ*, *Pd-l1*$^{-/-}$*+IFN-γ* and *WT+PD-L1*. n = 3. ***P < 0.001.

from PD-L1 overexpressing SK-MEL-5 cells were first stained with Cyanine5.5 NHS ester dye to reveal the appearance as small-red dots under confocal microscope (Figure 2(a)). As expected, pre-stained exosomes derived from PD-L1 overexpressing SK-MEL-5 cells colocalized with exogenous GFP-PD-1 on the cell membrane of HEK 293T cells (Figure 2(b)), as well as endogenous PD-1 on the Jurkat T cell surface (Figure 2(c)). As exosomal PD-L1 levels have been associated with immunosuppression in tumour microenvironment [17,31–33], we next asked whether exosomal PD-L1 could function similarly to cell-surface PD-L1 in the suppression of T cell activation. We confirmed that exosomes derived from IFN-γ treated cells (*WT+IFN-γ, Pd-l1*$^{-/-}$*+IFN-γ*) inhibited the proliferation of PBMCs to a similar level to FK506, a common immunosuppressive drug to inhibit T cell activation, as demonstrated by the decreased proportion of cells containing diluted CFSE (Figure 2(d)). In comparison, exosomes derived from SK-MEL-5 cells expressing exogenous PD-L1 (*WT+PD-L1*) inhibited the proliferation of PBMCs to a more dramatic extent, whereas control *WT* and *Pd-l1*$^{-/-}$ exosomes had no effect on T cell proliferation compared to control (*Ctrl (d3)*) (Figure 2(d)). A more dramatic difference was observed between exosomes derived from IFN-γ treated cells (*Pd-l1*$^{-/-}$*+IFN-γ*) and PD-L1 overexpressing cells (*WT+PD-L1*) when compared to the control cells with greater rounds of proliferation (7 days), further supporting that the major immune inhibitory effects of exosomes come from PD-L1 rather than other immune-related proteins in exosomes (Figure 2(e)). To further test if this T cell inhibition would influence wound healing, we performed wound scratch assay of skin cells by testing conditional medium isolated from SK-MEL-5-derived exosomes incubated with PBMCs for 3 days (Figure 2(f,g)). Interestingly, exosomal PD-L1 (*WT+PD-L1* and *WT+IFN-γ* groups) significantly enhanced the migration of both HaCaT keratinocytes and human dermal fibroblast (HDF) cells, to a similar level to induction of bFGF, a common growth factor to promote skin cell activities (Figure 2(f,g)). These data suggest that exosomal PD-L1 also regulate epidermal and dermal cellular processes that are required for skin repair.

Sustained release of exosomes from PF-127 hydrogel

In order to improve the therapeutic effects of exosomes, we incorporated exosomes into PF-127 hydrogel to release exosomes to the surroundings in a sustained manner [34]. First, we evaluated gel dissolution, as it is an important process for exosomes release. At a 20% PF-127 concentration, the solution–gel transition temperature is 24°C, which means that the polymer is in a solution state at low temperature but solidified near body temperature (Figure 3(a)). Next, we confirmed the physical properties of PF-127 hydrogel by rheological measurements of the elastic modulus (G′) and viscous modulus (G″) with increasing temperature from 5°C to 40°C and showed that the phase transition of the PF-127 solution to the hydrogel happened when the temperature rose to around 17°C (Figure 3(b)). The SEM image of PF-127 hydrogel morphology showed the average mesh size of about 4 μm (Figure 3(c)), providing a significant advantage for *in vivo* injection. To check if PF-127 hydrogel could improve the retention and stability of exosomes *in vitro*, 10 μg of WGA 488A-labelled exosomes were incorporated with 200 μL PF-127 hydrogel and gelatinized at 37°C. After keeping in a humidified incubator at 37°C for various times, we assessed the stability of hydrogel-incorporated exosomes by quantitating GFP signals at different time points (Figure 3(d,e)). With the increase of co-incubation time, the GFP signal gradually increases, with the peak time of 24 h incubation, and then slowly decreased (Figure 3(d,e)), suggesting exosomes are constantly released from PF-127 hydrogel into the surrounding cells.

Exosomal PD-L1 promotes skin wound healing in vivo

Based on observations in cellular models relevant to the wound-healing process, we would like to investigate whether exosomal PD-L1 is an important determinant of wound healing in a physiological environment. Thus, we made full-thickness excisional injury (10 mm in diameter) in mouse dorsal skin. Given the relatively small body surface area of this type of mice, the wound is much larger than standardized size, causing stronger and longer inflammation and making the wound more challenging to heal. Negative group was treated with 20% PF-127 alone (*Ctrl*), 20% PF-127 containing bFGF cytokine (*bFGF*), as well as 20% PF-127 containing exosomes derived from mouse melanoma B16F10 cell line (*WT, WT+PD-L1, WT+IFN-γ* groups) have been applied on top of the wounds over the 10 days. We found upon exosomal PD-L1 treatment, wounds (*WT+IFN-γ* and *WT+PD-L1* groups) almost healed from surface at day 10 post injury, whereas the epithelium layer in control mice (*WT* and *Ctrl* groups) was still covered by a large scab (Figure 4(a)). Furthermore, there was a faster wound closure in *WT+IFN-γ* group and *WT+PD-L1* group similar to positive *bFGF* group. We further compared the wound size and found that *WT+PD-L1* and *WT+IFN-γ*

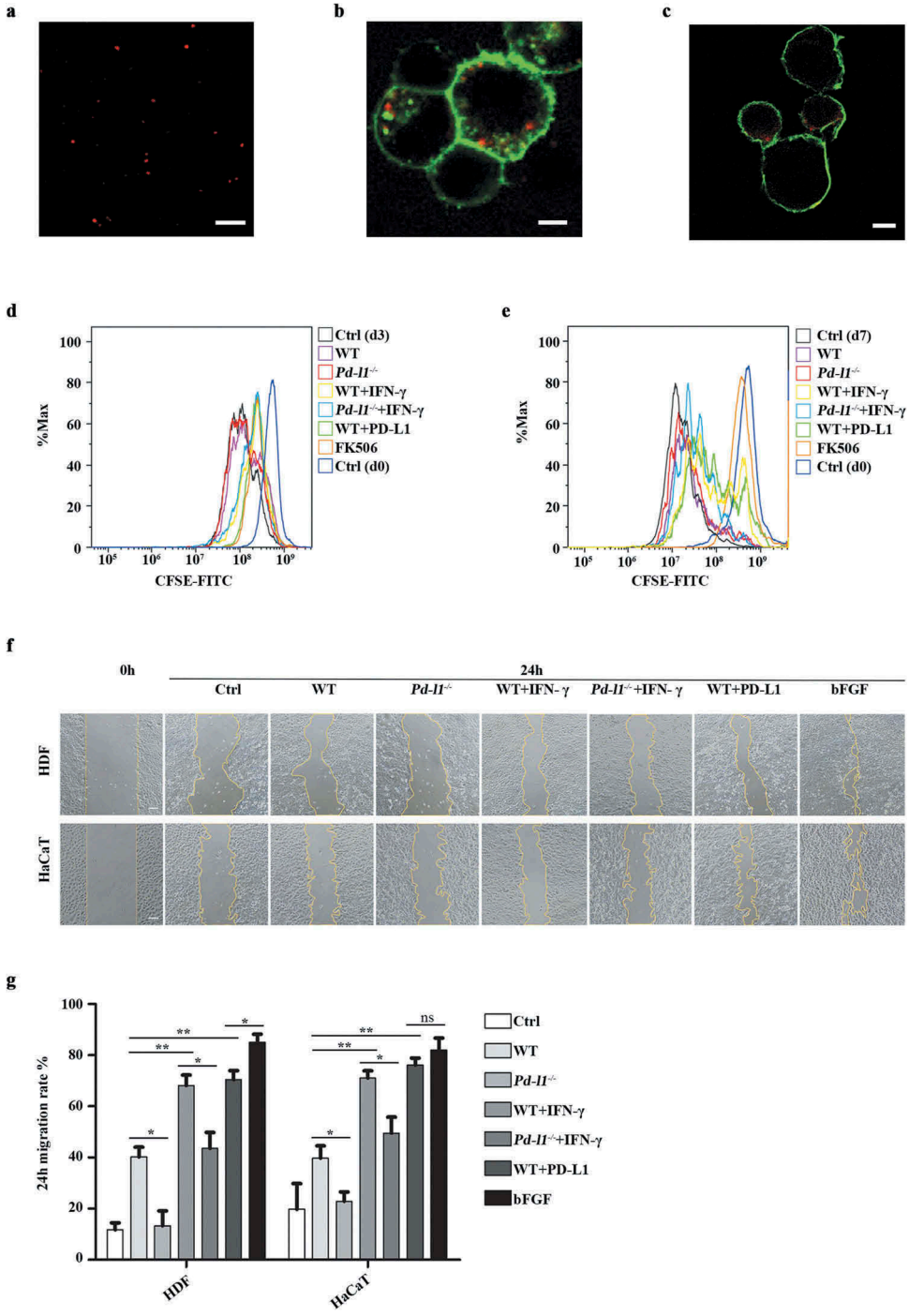

Figure 2. Exosomal PD-L1 suppressed T cell activation and promoted skin cell migration in vitro (a). Representative confocal image showed the appearance of exosomes as small-red dots. Scale bar: 5 μm. (b-c). Representative confocal images of pre-stained exosomes (red) colocalized with cell membrane (green) of HEK 293T (b) and Jurkat T cells (c). Scale bar: 5 μm. (d-e). Flow cytometry analysis of CFSE-labelled T cell proliferation assay. PBMCs (8×10^5) were incubated with *WT* (100 μg/mL)), *Pd-l1*$^{-/-}$ (100 μg/mL), *WT +IFN-γ* (100 μg/mL), *Pd-l1*$^{-/-}$*+IFN-γ* (100 μg/mL), *WT+PD-L1* (100 μg/mL) and *FK506* (100 nM) for 3 days and 7 days. Cells were cultured with mock reagents for 0, 3 and 7 days as *Ctrl (d0), Ctrl (d3)* and *Ctrl (d7)*, respectively. (f-g). Wound scratch assay of HDF cells and HaCaT cells. Wounded cells were incubated with *WT* (100 μg/mL), *Pd-l1*$^{-/-}$ (100 μg/mL), *WT+IFN-γ* (100 μg/mL), *Pd-l1*$^{-/-}$*+ IFN-γ* (100 μg/mL), *WT+PD-L1* (100 μg/mL) and *bFGF* (2.5 ng/mL) for 24 h. Serum-free medium was used as control (*Ctrl*). 24 h migration rate (g) and representative wound images (f) of each group at 24 h were shown. Scale bar: 100 μm. n = 3. *P < 0.05; **P < 0.01; ns, not significant.

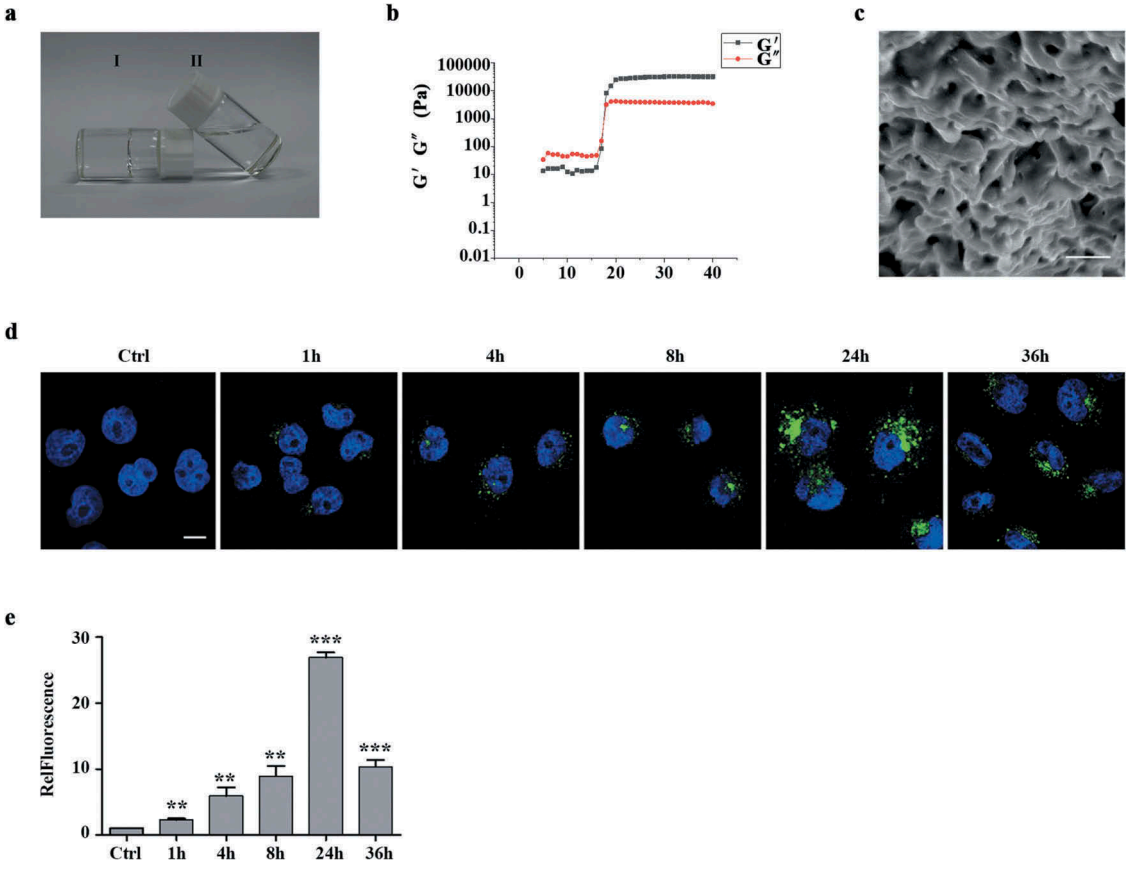

Figure 3. Characterization of the exosomes released from the thermoresponsive hydrogel PF-127 (a). The state of 20% PF-127 hydrogel changes as temperature changes. I and II represent PF-127 hydrogel (room temperature) and PF-127 solution (4 °C), respectively. (b). The image showed dynamic storage modulus (G′) and loss modulus (G″) change by a heating rate of 5°C/min from 5°C to 40°C. (c). SEM image of 20% PF-127 hydrogel. Scale bar: 5 μm. (d). Representative confocal images of exosomes uptake by recipient HaCaT cells were provided at 0, 4, 8, 24 and 36 h. Green, exosomes staining with WGA 488A dye. Blue, nuclear staining with DAPI. Scale bar: 10 μm. (e). Quantification of exosome uptake shown as mean fold changes (± SEM) by HaCaT cells. n = 3. RelFluorescence, relative fluorescence. **P < 0.01; ***P < 0.001.

groups had smaller wounds than *WT* group over 10 days of wound healing (Figure 4(b)), demonstrating that exosomal PD-L1 leads to a faster recovery of the tissue. A histological analysis of wound morphology 7 days after injury revealed a statistically significant reduction of inflammation and immune cell infiltration, together with enhanced re-epithelialization in *WT+IFN-γ* and *WT+PD-L1* groups compared to *WT* and *Ctrl* groups (Figure 4(c)). Immunohistochemistry analysis with α-SMA, vimentin and Ki67 antibodies also revealed that migration, maturation, and proliferation in epidermis and dermis all speeded up in the PD-L1 group, which are prerequisites for proper wound healing (Figure 4(c)). Next, we investigated the immune signalling in wounded regions. qPCR analysis showed lower mRNA level of IL6, TNF-a, granzyme B levels in *WT+IFN-γ* and *WT+PD-L1* groups compared to *WT or bFGF* group (Figure 4(d)). Interestingly, *Ctrl* group had stronger inflammation and production of immune cytokines, suggesting a protective role of PF-127 hydrogel against infection and inflammation (Figure 4(d)). Consistently, flow cytometry analysis revealed less CD8+ T cells in the lymph nodes, but not in the spleens in *WT+IFN-γ* and *WT+PD-L1* groups when compared to control *WT* group, indicating that regional application of PD-L1-high exosomes to the injured sites has a negative effect on T cell activation in nearby peripheral lymphatic tissues, but not on distant lymphatic organs such as spleen (Figure 4(e,h)).

Discussion

In this study, we present results of exosomal PD-L1 binding to PD-1 in T cell surface as well as enhancing excisional wound healing upon large skin injury. We also found that exosomes carrying cargos can be embedded into a novel thermoresponsive gel on top of the injured skin, providing a new perspective for using immunotherapy to promote tissue repair and regeneration.

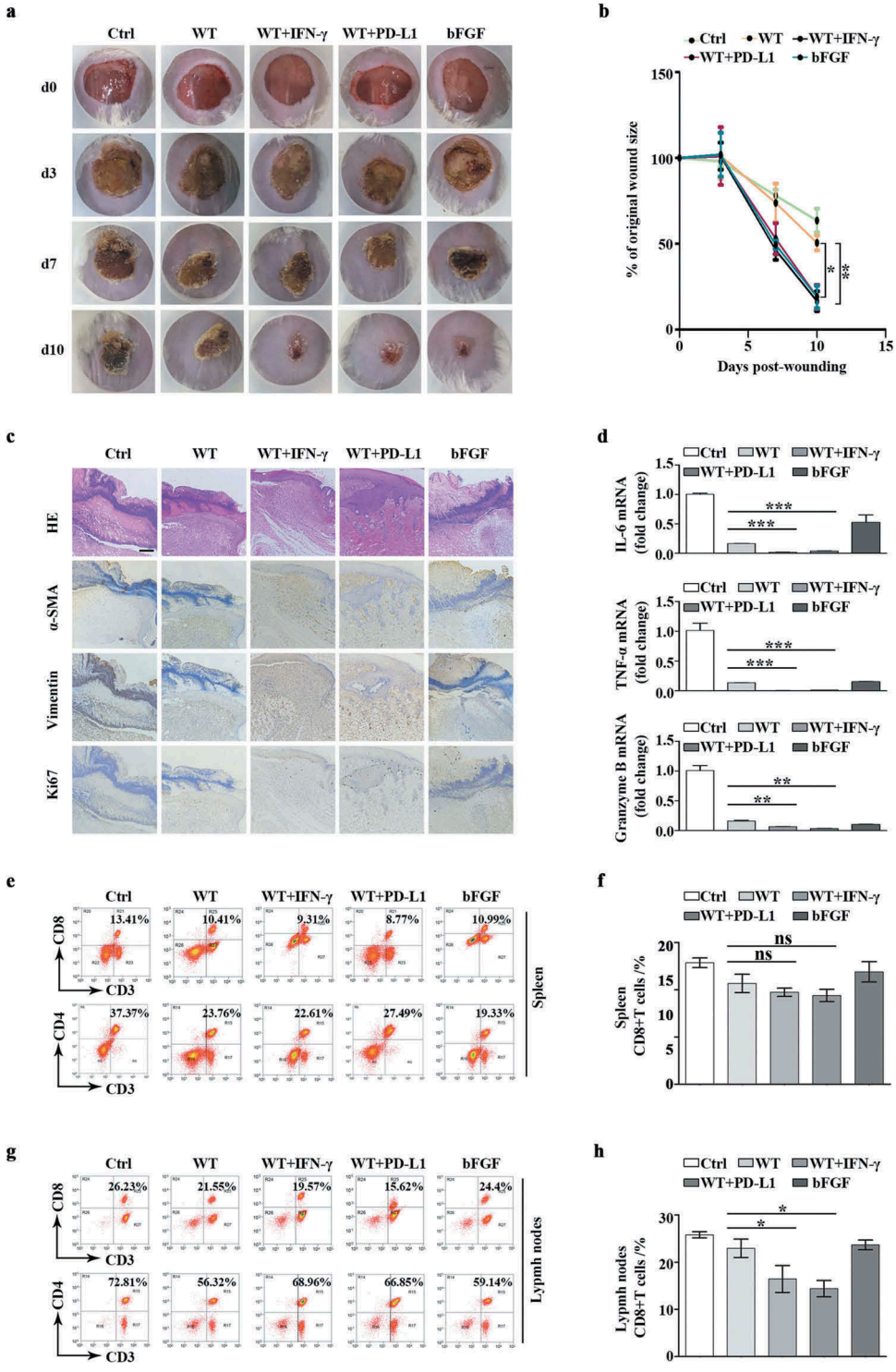

Figure 4. Exosomal PD-L1 accelerated mouse skin wound closure (a). Representative wound images from mice treated with 20% PF-127 alone (*Ctrl*), treated with 20% PF-127 containing bFGF cytokine (*bFGF*), or 20% PF-127 containing exosomes (*WT, WT+PD-L1, WT +IFN-γ*) over 10 days of healing period. The same ring was used to compare the size of all wounds. (b). Comparison of the percentages of the open wound size over 10 days healing period between *Ctrl, WT, WT+IFN-γ, WT+PD-L1* and *bFGF* groups. n = 3. (c). Representative histological images (HE) and immunohistochemical images for vimentin, α-SMA and Ki67 antibodies in the wounds on day 7. Scale bar: 200 μm. (d). qPCR of IL-6, TNF-α, granzyme B mRNA levels in the wounded skin on day 7 from different groups. n = 3. (e-h). Representative flow cytometry plots demonstrated change of CD4+ and CD8 + T cells (gated on positive CD3+ cells) in spleen (e) and peripheral lymph nodes (g) on day 7 of wound healing. (f) and (h) were quantitation from (e) and (g). n = 2–3. *P < 0.05; **P < 0.01; ***P < 0.001; ns, not significant.

A continuing inflammatory process disrupts immune function by focusing the immune system on the affected area. It is characterized by a continuing leukocyte (and macrophage) infiltration that release cytotoxic enzymes, free radicals, and inflammatory mediators that cause extensive tissue damage [7,8]. Thus, it is suggested to reduce the inflammatory immune response in order to speed up healing and improve the final scar appearance. In this study, we focused on PD-1/PD-L1 immune checkpoint pathway of T cells during the inflammation phase of healing. It is necessary to investigate how other immune inflammatory signalling pathways (CTLA-4/CD80, TIM3-Galectin9) regulate wound healing in depth [35–38].

Exosomes have emerged as a drug delivery nanoplatform, and in this study, we loaded exogeneous PD-L1 into cells to successfully generate high concentration of exosomal PD-L1, which confers enhanced function and targeting capability as a potential therapeutic cargo in cutaneous wound healing. These exosomes, derived from genetically engineered cells overexpressing PD-L1, function similarly to exosomes from cytokine-stimulated cells in negatively regulating T cell activity.

In order to increase the inflammation around the skin wound and slow down the healing speed in the mouse model, we created large cutaneous wounds (diameter = 10 mm) on the mouse dorsal skin, and no wound dressings or other topical protective procedures were applied to the affected area. In order to reduce the potential infection risk derived from anti-inflammatory therapies, we have used a couple of measures including: (1) the major targeting cells of PD-L1-exosomes are cytotoxic T cells, not neutrophils or macrophages which are major inflammatory cells infiltrating to the wounds to fight against microbial infection right after injury; (2) Exosome treatment was started on day 3 post injury, as the inflammation occurs immediately following the injury, and the first 3 days in inflammation phase were crucial for inflammatory and immune cells to clear cell debris and infection; 3) we used the thermoresponsive hydrogel system to release exosomes, which performed properties of rapid self-healing and acted as a barrier between the wound and the outside environment against microbial infections. Nonetheless, this cutaneous wound model has its limitation as other types of injuries such as incisional and burn wound models are slightly different in physiopathological conditions and underlying molecular mechanisms. Furthermore, in this study, we used an acute excisional wound healing model rather than a chronic model, in which exosomal PD-L1 may have even stronger effect in controlling immune inflammatory process. In the future, diabetic or psoriasis mouse models can be used to explore the impact of immune signalling pathways on chronic inflammatory microenvironment.

In summary, we described a new finding of exosomal PD-L1 functional as immunosuppressants. This could be promising cell-free therapies promoting tissue repair and regeneration, which will provide a theoretical and experimental basis for new immunotherapy to treat organ transplantation rejection, autoimmune diseases, chronic infection, post-injury chronic inflammation and beyond.

Disclosure of interest

The authors report no conflict of interest.

Funding

This work was supported by the National Natural Science Foundation of China [81702750, 81670141, 81970145, 81502663]; Science, Technology & Innovation Commission of Shenzhen Municipality [JCYJ20170818164756460, JCYJ 20180307154700308, JCYJ20170818163844015, JCYJ2018030 7151420045]; China Postdoctoral Science Foundation [2018M643299, 2018M631033]; The Social Development Foundation of Jiangsu Province [BE2018691]; Six talent peals project of Jiangsu Province [WSW-039] and Sigrid Jusélius Stiftelse, Finland.

References

[1] Rodrigues M, Kosaric N, Bonham CA, et al. Wound healing: a cellular perspective. Physiol Rev. 2019;99 (1):665–706.
[2] Eming SA, Martin P, Tomic-Canic M. Wound repair and regeneration: mechanisms, signaling, and translation. Sci Transl Med. 2014;6(265):16.
[3] Gurtner GC, Werner S, Barrandon Y, et al. Wound repair and regeneration. Nature. 2008;453(7193):314–321.
[4] Blakytny R, Jude E. The molecular biology of chronic wounds and delayed healing in diabetes. Diabetic Med. 2006;23(6):594–608.
[5] Grey JE, Harding KG, Enoch S. Venous and arterial leg ulcers. BMJ. 2006;332(7537):347–350.
[6] Martin P, Nunan R. Cellular and molecular mechanisms of repair in acute and chronic wound healing. Br J Dermatol. 2015;173(2):370–378.
[7] Behm B, Babilas P, Landthaler M, et al. Cytokines, chemokines and growth factors in wound healing. J Eur Acad Dermatol Venereol. 2012;26(7):812–820.
[8] Eming SA, Wynn TA, Martin P. Inflammation and metabolism in tissue repair and regeneration. Science. 2017;356(6342):1026–1030.
[9] Karin M, Clevers H. Reparative inflammation takes charge of tissue regeneration. Nature. 2016;529 (7586):307–315.

[10] Martin P, Leibovich SJ. Inflammatory cells during wound, repair: the good, the bad and the ugly. Trends Cell Biol. 2005;15(11):599–607.
[11] ELA S, Mager I, Breakefield XO, et al. Extracellular vesicles: biology and emerging therapeutic opportunities. Nat Rev Drug Discov. 2013;12(5):347–357.
[12] Kowal J, Tkach M, Thery C. Biogenesis and secretion of exosomes. Curr Opin Cell Biol. 2014;29:116–125.
[13] Tkach M, Thery C. Communication by extracellular vesicles: where we are and where we need to go. Cell. 2016;164(6):1226–1232.
[14] Buzas EI, Gyorgy B, Nagy G, et al. Emerging role of extracellular vesicles in inflammatory diseases. Nat Rev Rheumatol. 2014;10(6):356–364.
[15] Whiteside TL. Exosomes and tumor-mediated immune suppression. J Clin Invest. 2016;126(4):1216–1223.
[16] Robbins PD, Dorronsoro A, Booker CN. Regulation of chronic inflammatory and immune processes by extracellular vesicles. J Clin Invest. 2016;126(4):1173–1180.
[17] Chen G, Huang AC, Zhang W, et al. Exosomal PD-L1 contributes to immunosuppression and is associated with anti-PD-1 response. Nature. 2018;560(7718):382–386.
[18] Muller L, Mitsuhashi M, Simms P, et al. Tumor-derived exosomes regulate expression of immune function-related genes in human T cell subsets. Sci Rep. 2016;6:20254.
[19] Syn NL, Wang L, Chow EK, et al. Exosomes in cancer nanomedicine and immunotherapy: prospects and challenges. Trends Biotechnol. 2017;35(7):665–676.
[20] Riella LV, Paterson AM, Sharpe AH, et al. Role of the PD-1 pathway in the immune response. Am J Transplant. 2012;12(10):2575–2587.
[21] Yang WH, Chen PW, Li HC, et al. PD-L1: PD-1 interaction contributes to the functional suppression of T-cell responses to human uveal melanoma cells in vitro. Invest Ophthalmol Vis Sci. 2008;49(6):2518–2525.
[22] Ritprajak P, Azuma M. Intrinsic and extrinsic control of expression of the immunoregulatory molecule PD-L1 in epithelial cells and squamous cell carcinoma. Oral Oncol. 2015;51(3):221–228.
[23] Poggio M, Hu T, Pai CC, et al. Suppression of exosomal PD-L1 induces systemic anti-tumor immunity and memory. Cell. 2019;177(2):414–427 e413.
[24] Boussiotis VA, Longo DL. Molecular and biochemical aspects of the PD-1 checkpoint pathway. N Engl J Med. 2016;375(18):1767–1778.
[25] Spranger S, Spaapen RM, Zha Y, et al. Up-regulation of PD-L1, IDO, and T(regs) in the melanoma tumor microenvironment is driven by CD8(+) T cells. Sci Transl Med. 2013;5(200):200ra116.
[26] Francisco LM, Salinas VH, Brown KE, et al. PD-L1 regulates the development, maintenance, and function of induced regulatory T cells. J Exp Med. 2009;206(13):3015–3029.
[27] Bertrand F, Montfort A, Marcheteau E, et al. TNFα blockade overcomes resistance to anti-PD-1 in experimental melanoma. Nat Commun. 2017;8(1):2256.
[28] Wu X, Zhang H, Xing Q, et al. PD-1(+) CD8(+) T cells are exhausted in tumours and functional in draining lymph nodes of colorectal cancer patients. Br J Cancer. 2014;111(7):1391–1399.
[29] Doench JG, Fusi N, Sullender M, et al. Optimized sgRNA design to maximize activity and minimize off-target effects of CRISPR-Cas9. Nat Biotechnol. 2016;34(2):184–191.
[30] Thery C, Amigorena S, Raposo G, et al. Isolation and characterization of exosomes from cell culture supernatants and biological fluids. Curr Protoc Cell Biol. 2006;30: 3.22.1–3.22.29. Chapter 3 Unit 3.22.
[31] Theodoraki MN, Yerneni SS, Hoffmann TK, et al. Clinical significance of PD-L1(+) exosomes in plasma of head and neck cancer patients. Clin Cancer Res. 2018;24(4):896–905.
[32] Yang Y, Li CW, Chan LC, et al. Exosomal PD-L1 harbors active defense function to suppress T cell killing of breast cancer cells and promote tumor growth. Cell Res. 2018;28(8):862–864.
[33] Ricklefs FL, Alayo Q, Krenzlin H, et al. Immune evasion mediated by PD-L1 on glioblastoma-derived extracellular vesicles. Sci Adv. 2018;4(3):14.
[34] Silva AKA, Perretta S, Perrod G, et al. Thermoresponsive gel embedded with adipose stem-cell-derived extracellular vesicles promotes esophageal fistula healing in a thermo-actuated delivery strategy. ACS Nano. 2018;12(10):9800–9814.
[35] Walker LSK, Sansom DM. The emerging role of CTLA4 as a cell-extrinsic regulator of T cell responses. Nat Rev Immunol. 2011;11(12):852–863.
[36] Rowshanravan B, Halliday N, Sansom DM. CTLA-4: a moving target in immunotherapy. Blood. 2018;131(1):58–67.
[37] Dardalhon V, Anderson AC, Karman J, et al. Tim-3/Galectin-9 Pathway: regulation of Th1 immunity through promotion of CD11b(+)Ly-6G(+) myeloid cells. J Iimmunol. 2010;185(3):1383–1392.
[38] Anderson AC, Anderson DE, Bregoli L, et al. Promotion of tissue inflammation by the immune receptor Tim-3 expressed on innate immune cells. Science. 2007;318(5853):1141–1143.